Electronic states and adhesion properties at metal/MgO incoherent interfaces: First-principles calculations

Daisuke Matsunaka* and Yoji Shibutani
Center for Atomic and Molecular Technologies and Department of Mechanical Engineering, Osaka University, Osaka 565-0871, Japan
(Received 3 February 2008; revised manuscript received 31 March 2008; published 30 April 2008)

We investigate interface structure and adhesion behavior of incoherent metal/oxide interfaces with large misfit, Cu/MgO(001) and Ni/MgO(001), based on the density functional theory. We show that the interfacial strain and bonding characteristics are inhomogeneous, depending on local atomic configurations at the incoherent interfaces. In regions where a metal atom is located near an O atom, the interfacial metal layer is stretched to the coherent positions and the metal-O interfacial bond has a covalent and ionic bonding character. On the other hand, in regions where a metal atom is situated near a Mg atom, the metal layer is hardly strained and the atomic geometry remains incoherent. The metal-Mg adhesive interaction is mediated by the image-charge electron accumulation, which is absent in the coherent interface model results. We also find that effects of the interfacial strain as well as the metal-Mg interaction on the adhesive energy are significant for accurate estimation of the stability of incoherent metal/oxide interfaces.

DOI: 10.1103/PhysRevB.77.165435 PACS number(s): 73.20.−r, 68.35.Np

I. INTRODUCTION

Metal/oxide interfaces are important components in advanced applications, such as microelectronics devices, photovoltaic devices, composites, coatings, sensors, catalysts, etc.[1–3] The functions and properties of metal/oxide interfaces play a key role in the performance of such applications. Moreover, the metal/oxide interface must possess the adequate thermodynamic mechanical stability under the particular conditions of the application. Understanding stability and adhesion properties of the interfaces is one of the most important issues in current material research. Interface structure and adhesion behavior of metal/oxide interfaces have so far been investigated by first-principles calculations. Although it is generally difficult to describe electronic states at the interface between dissimilar materials, simply by a particular chemical bonding, such as metallic and ionic, first-principles calculation assuming no *a priori* type of chemical bonding is a useful method to investigate electronic states at the interface. In current first-principles studies, two complementary approaches are used for quantum mechanical modeling of interfaces: a small cluster of atoms and a periodic slab of crystal layers. The first-principles calculations using a cluster model[4–10] have accurately provided the adsorption energy and bonding strength of adatom or cluster deposited on the oxide surface, in qualitatively agreement with experiments,[11–14] though the adsorption energy is dependent on the method of calculation and the appropriate functional should be chosen. Several comprehensive studies classified the adsorption behavior among transition metals.[6] On the other hand, based on the periodic slab model, typical features of an interface between a bulk metal and a bulk oxide have been investigated.[15–18] The periodic slab model represents an interface as a sandwich of semi-infinite crystal layers and can take account of the metallic binding character. Almost exclusively in previous calculations, however, the coherent interface approximation is imposed in the supercell, i.e., the change in the lattice constant across heterophase interfaces is neglected, and thus effects of misfit are not adequately evaluated. While Ag/MgO is a model system as the coherent interface, most of metal/oxide interfaces are incoherent with misfit. Recently, Benedek *et al.* carried out first-principles calculations of Cu/MgO{222}, including lattice constant mismatch by extending metal and oxide layers of slab, parallel to interface.[19] Matsunaga *et al.* also calculated Ni/ZrO_2(111) interface with a similar extended supercell of the incoherent interface.[20] They have shown that the bonding nature at the incoherent interface is strongly dependent on local atomic configurations which the lattice misfit gives rise to. Unfortunately, there are only a few cases of incoherent metal/oxide interface calculated in such a manner, and the physical origin of adhesion in incoherent metal/oxide interfaces is in controversy.

In this study, we carry out first-principles calculations of incoherent metal/oxide interfaces, Cu/MgO(001) and Ni/MgO(001), based on the density functional theory (DFT). Among metal/oxide interfaces, the metal/MgO(001) interface is one of the most studied systems, mainly because the MgO(001) surface structure is simple, stoichiometric, and stable. The observed orientation relationships of these interfaces are (001)metal‖(001)MgO and [100]metal‖[100]MgO.[13,21,22] In order to consider the large misfit of incoherent interfaces, we adopt the coincidence boundary slab model by extending the supercell parallel to interface.[19,20] While the difference in lattice constant can be described in the extended interface supercell, the computation time increases as a function of the third power of the number of atoms in the supercell. Cu/MgO and Ni/MgO are feasible for such modeling of interface, because each lattice constant mismatch is approximately represented by a simple ratio. We focus on interface structure and adhesion behavior of the incoherent metal/oxide interfaces with large misfit, although it is important to elucidate the functional properties, such as high catalytic activity of metal clusters supported on oxide surfaces. Our DFT results demonstrate that interfacial strain and bonding characteristics are inhomogeneous at incoherent interfaces, depending on local atomic configurations. We also show that effects of the inhomogeneity are

significant for accurate evaluation of the stability of incoherent metal/oxide interfaces, by comparing with results within the coherent interface approximation.

II. METHODS

The metal/oxide interface systems of Cu/MgO(001) and Ni/MgO(001) are modeled using a slab geometry with three metal and three MgO layers. Our calculated values of the lattice constant of Cu, Ni, and MgO bulks are a^0_{Cu}=3.64 Å, a^0_{Ni}=3.52 Å, and a^0_{MgO}=4.24 Å, respectively. For these interfaces, the misfit parameter defined by $\delta=(ma^0_{\mathrm{MgO}}-na^0_{\mathrm{Me}})/ma^0_{\mathrm{MgO}}$ is large, but the ratio of the metal and oxide lattice constants can be approximated by a simple ratio; $7a^0_{\mathrm{Cu}}\sim 6a^0_{\mathrm{MgO}}$ for Cu/MgO(001) and $6a^0_{\mathrm{Ni}}\sim 5a^0_{\mathrm{MgO}}$ for Ni/MgO(001). In order to consider their large misfit, we adopt the coincidence boundary slab for the incoherent metal/oxide interface. The supercell is extended parallel to the interface, so as to be consistent with both the crystal lattice periods of metal and MgO layers.[19,20] For Cu/MgO(001), the Cu layer contains 7×7 atoms and the MgO layer consists of 6×6 atoms, in the extended supercell. Likewise, for Ni/MgO(001), the Ni and MgO layers contain 6×6 and 5×5 atoms, respectively. The difference of lateral repeat units of metal and oxide layers is negligible in the extended supercell. As the interface geometry is inhomogeneous, the incoherent interface contains various types of interfacial atomic configuration. We compare the DFT results using the incoherent interface models, i.e., the coincidence boundary slabs in the extended supercells, with the DFT calculations using the coherent interface model where metal layers are stretched to the lattice constant of MgO layer. The coherent interface model represents the interface structure by a particular atomic configuration. We consider here two types of the coherent interface configuration, where metal atoms sit on either surface O or Mg atoms, denoted as O-atop and Mg-atop, respectively.

The electronic structure calculations of the interface system, based on DFT, are performed using the projector augmented wave method[23,24] as implemented in the *ab initio* total-energy and molecular-dynamics program VASP.[25] The spin polarization is considered in the calculations of the systems containing Ni atoms. The exchange-correlation potential is calculated within the generalized gradient approximation using the Perdew-Wang parametrization.[26] The plane-wave basis set is limited with an energy cutoff of 400 eV. The Brillouin zone is sampled only at the Γ point for the incoherent interface model, while using a $6\times6\times1$ Monkhorst-Pack mesh for the coherent interface model.[27] The geometry optimization is achieved until the forces on all the unconstrained atoms are smaller than 0.02 eV/Å, while the bottom MgO layer is fixed to the bulk position.

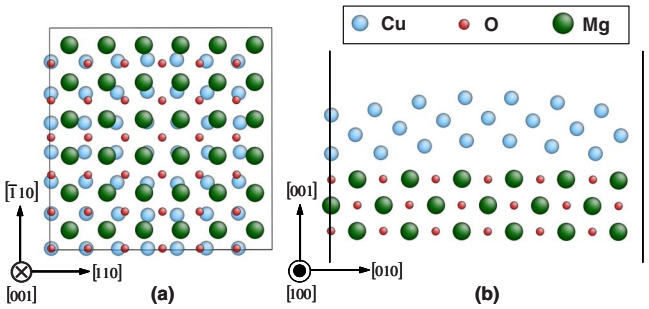

FIG. 1. (Color online) Relaxed Cu/MgO(001) interface structure. (a) Interfacial atomic geometry of Cu and MgO layers adjacent to the interface and (b) cross-sectional side view of the interface structure from the [100] direction corresponding to that diagonal line in (a). The lateral repeat units of the extended supercell are indicated by the solid lines.

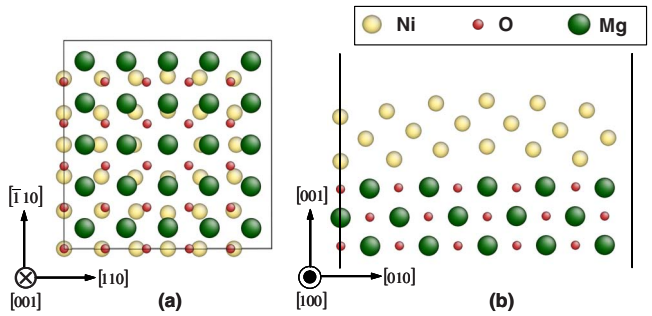

FIG. 2. (Color online) Relaxed Ni/MgO(001) interface structure. (a) Interfacial atomic geometry of Cu and MgO layers adjacent to the interface and (b) cross-sectional side view of the interface structure from the [100] direction corresponding to that diagonal line in (a). The lateral repeat units of the extended supercell are indicated by the solid lines.

III. RESULTS AND DISCUSSION

The optimized atomic geometries of the Cu/MgO(001) and Ni/MgO(001) interfaces are shown in Figs. 1 and 2, respectively. The relaxation of each atom, relative to perfect crystals, is inhomogeneous, depending on local atomic configurations at the interface. A metal atom (Cu or Ni in the present study) in the vicinity of an O atom relaxes into the O-atop coherent configuration where the metal atom is located just above the O atom. At the O-atop site, the interatomic distance in the interfacial metal layer is stretched to about 13% for Cu/MgO and about 10% for Ni/MgO. The metal atom is strongly attracted onto the O atom, despite the large misfit strain. On the other hand, a metal atom adhered nearly above a Mg atom does not remarkably relax. The interatomic distance in the metal layer is hardly strained in

TABLE I. Interfacial bond lengths of Cu/MgO(001) and Ni/MgO(001).

		Bond length (Å)	
	Model	Metal-O	Metal-Mg
Cu/MgO(001)	Incoherent	2.10	3.05
	Coherent	2.16	3.24
Ni/MgO(001)	Incoherent	2.01	2.88
	Coherent	2.02	3.36

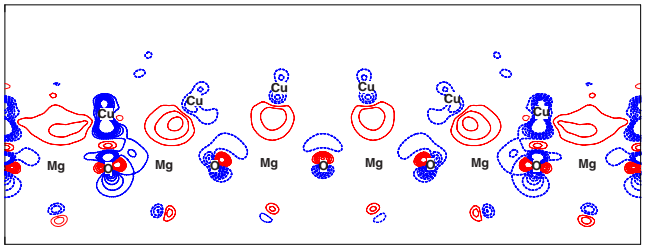

FIG. 3. (Color online) Difference electron density map for the Cu/MgO(001), on the (100) plane as well as Fig. 1(b). The contour lines are drawn from −0.07 to 0.07 with an interval of 0.01 in electrons/Å^2, except for the zero contour line. The solid and broken lines correspond to the positive and negative values, respectively. The positions of the interfacial atoms on this cross section are indicated.

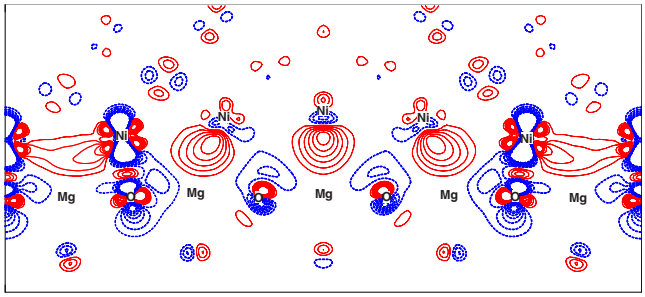

FIG. 4. (Color online) Difference electron density map for the Ni/MgO(001), on the (100) plane as well as Fig. 2(b). The contour lines are drawn from −0.07 to 0.07 with an interval of 0.01 in electrons/Å^2, except for the zero contour line. The solid and broken lines correspond to the positive and negative values, respectively. The positions of the interfacial atoms on this cross section are indicated.

the Mg-atop region of the interface. The bond length across the interface is also dependent on the local atomic configuration. As shown in Table I, the interfacial bond length at the O-atop site is shorter than at the Mg-atop site, implying the stronger metal-O interaction. The metal-O bond lengths are comparable with the values obtained by the O-atop coherent interface models. It is because the atomic geometry at the O-atop site of the interface, where the metal layer is stretched, gets fairly coherent. Furthermore, the Ni–O bond length is shorter than the Cu–O bond length, qualitatively consistent with the cluster DFT calculations.[4,6,7,9,10] However, the metal-Mg bond length is smaller than the coherent interface model results. At the Mg-atop site of the interfaces, the metal layer is not strained and the incoherent atomic geometry due to misfit is retained. Thus, the electronic states in the Mg-atop region of the interfaces would be different from those obtained by the coherent interface models.

In order to investigate the bonding characteristics at the interfaces, the difference electron density due to adhesion is calculated, by subtracting the charge densities of isolated metal and MgO slabs having the same atomic positions with the interface supercells from that of the interface. The countermaps illustrate how the valence electrons are redistributed

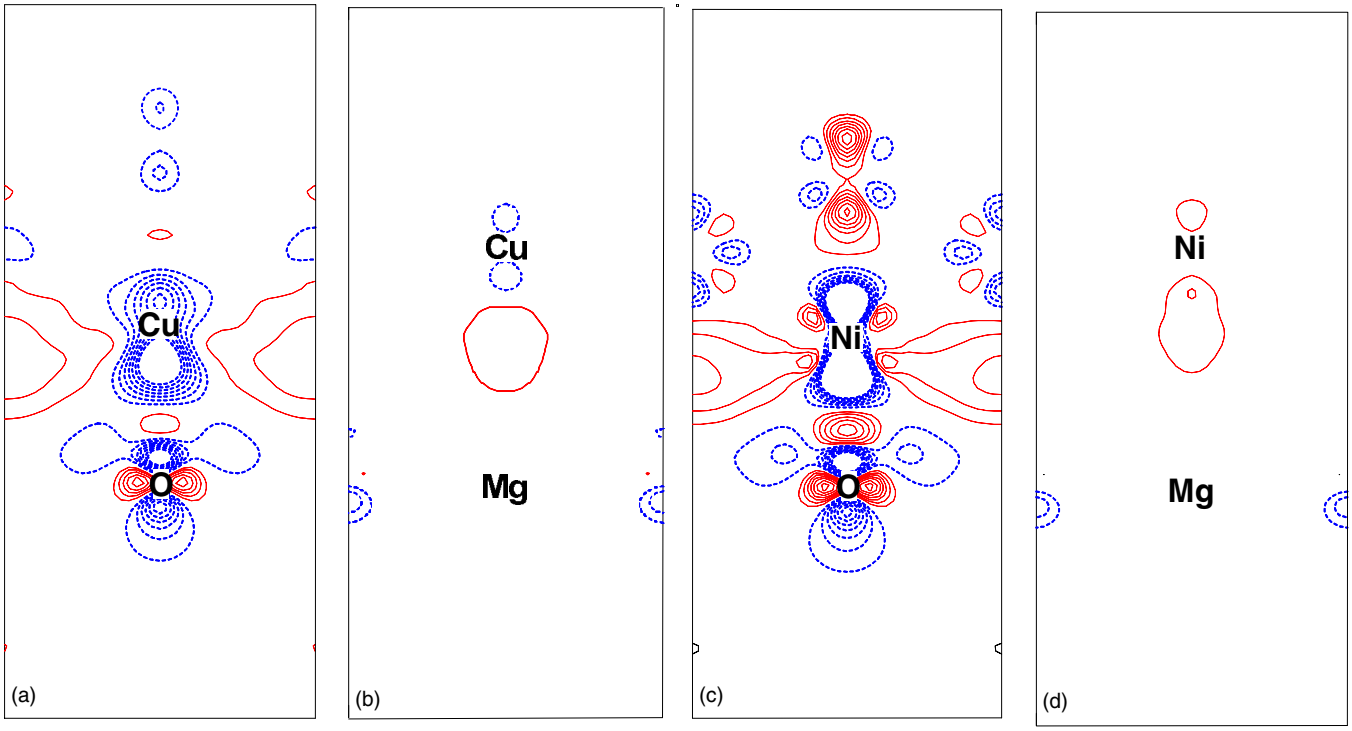

FIG. 5. (Color online) Difference electron density maps for the coherent interface models of Cu/MgO(001) [(a) and (b)] and Ni/MgO(001) [(c) and (d)], on the (100) plane. (a) and (c) correspond to the O-atop configuration interfaces, while (b) and (c) to the Mg-atop ones. The contour lines are drawn from −0.07 to 0.07 with an interval of 0.01 in electrons/Å^2, except for the zero contour line. The solid and broken lines correspond to the positive and negative values, respectively. The positions of the interfacial atoms on this cross section are indicated.

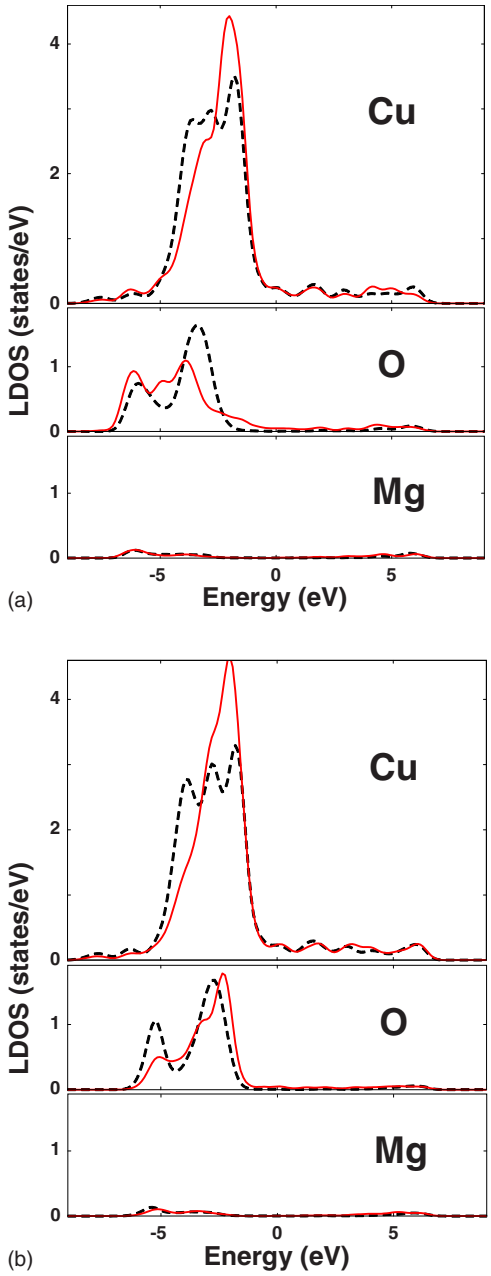

FIG. 6. (Color online) Local density of states for atoms at (a) O-atop and (b) Mg-atop sites of Cu/MgO(001). Projections on atoms of interfacial (solid lines) and second layers are plotted. The Fermi level is set at 0 eV.

to form adhesive bonds, and regions with any nonzero contour values attribute to adhesive interaction. In Figs. 3 and 4, the difference electron density maps are shown for Cu/MgO(001) and Ni/MgO(001), respectively. For both the interfaces, the difference electron density is effectively restricted within the interfacial metal and MgO layers, and depends on the local atomic configuration at the interface. This demonstrates the importance of the local atomic configuration to the incoherent metal-MgO adhesion. At the O-atop site, substantial and localized charge redistribution is established between the metal and O atoms, indicating strong covalent interaction. This covalent metal-O interaction is consistent with the adsorption behavior of metal atoms on MgO(001) surface, obtained by the cluster DFT calculations.[4–7,9] The Ni–O bond at Ni/MgO(001) exhibits more electron accumulation than the Cu–O bond at Cu/MgO(001), attributable to the incomplete 3*d* shell of Ni. In addition to the covalent character of the metal-O interaction, a broad charge redistribution occurs at the interstitial site between the O-atop metal atoms, i.e., above a Mg atom, as expected from the classical image-charge theory.[28,29] The accumulated electrons interact with the positively charged Mg atom in an ionic manner. Therefore, the adhesion behavior at the O-atop site has a partly covalent and ionic bonding characteristic. On the other hand, at the Mg-atop site, the image-charge ionic interaction is induced by the electrostatic field of MgO. The interfacial MgO layer no longer directly interacts with metal atoms, but the adhesion interaction is mediated by the image-charge electrons accumulated above the Mg atoms. Any covalentlike interaction is not observed in both the difference electron densities of Cu/MgO(001) and Ni/MgO(001).

In Fig. 5, we show difference electron density results obtained by the coherent interface model calculations. For the O-atop configuration, as well as in the results by the incoherent interface models, the partly covalent and ionic bonding feature appears. On the other hand, there are only minor charge redistributions for the Mg-atop configuration. The image-charge electron accumulation between the metal and Mg atoms is much less than in the results by the incoherent interface models. In significantly stretched metals, valence electrons tend to relatively bound near metal atoms due to the longer interatomic distance. This results in the suppression of the electron accumulation between the metal and Mg atoms.

As a complementary information on the electronic states at the interfaces, local densities of states (LDOSs) for the Cu/MgO(001) and Ni/MgO(001) are plotted in Figs. 6 and 7, respectively. The LDOS profiles for the interfacial atoms at the O-atop or Mg-atop sites and the interior atoms at the center of each slab are only shown. The LDOS shapes for the metal atoms above O and Mg atoms are similar, as both the metal-O and metal-Mg bonds are contributed by the image-charge interaction due to the electrostatic field of the ionic MgO layer. In the LDOS at the O-atop site, moreover, the interfacial states are visible below the metal *d* band and in the MgO band gap, reflecting the covalent metal-O interaction. The LDOS shape for the O atom at the O-atop site, bonded to the metal atom, is quite different from that for the interior O atom, indicating the strong metal-O interaction.

We estimate adhesive energy to form the interfaces with metal and MgO surfaces, by subtracting the energies calculated for metal and MgO surface slabs, $E_{\mathrm{adh}}=(E_{\mathrm{Me/MgO}}-E_{\mathrm{Me}}-E_{\mathrm{MgO}})/A_{\mathrm{int}}$. A_{int} is an interface area. The atomic structures of the metal and MgO surface slabs are optimized, and then the surface structures are not strained because the lateral repeat units of the extended supercell is consistent with both the crystal lattice periods of metal and MgO. Although the adhesive energy is not measurable directly, it is a useful measure of the stability of interface from a viewpoint of theoretical treatments. In the case of incoherent interfaces, the adhesive energy includes not only chemical bonding part E_c but

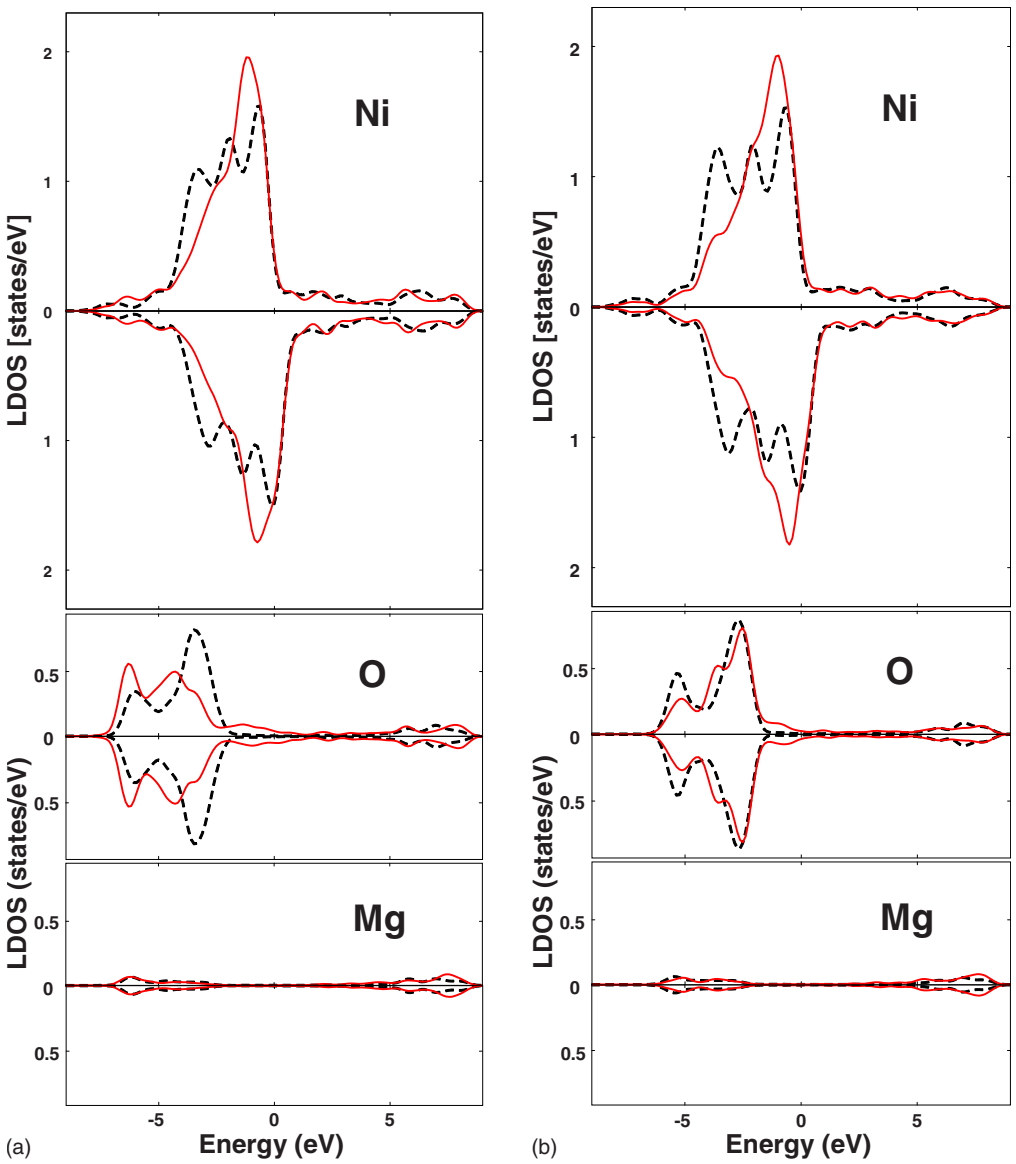

FIG. 7. (Color online) Spin-polarized local density of states for atoms at (a) O-atop and (b) Mg-atop sites of Ni/MgO(001). Projections on atoms of interfacial (solid lines) and second layers are plotted. The majority and minority spin states are shown in the upper and lower panels, respectively. The Fermi level is set at 0 eV.

interfacial strain contribution E_s. In the DFT studies with the coherent interface model, effects of E_s have been almost neglected. We divide E_{adh} into E_c and E_s with the energies calculated for the isolated metal and MgO slab, E^s_{Me} and E^s_{MgO}, as in the calculations of difference electron density, as follows:

$$E_{\mathrm{adh}} = E_c - E_s, \tag{1}$$

$$E_c = (E_{\mathrm{Me/MgO}} - E^s_{\mathrm{Me}} - E^s_{\mathrm{MgO}})/A, \tag{2}$$

$$E_s = (E^s_{\mathrm{Me}} + E^s_{\mathrm{MgO}} - E_{\mathrm{Me}} - E_{\mathrm{MgO}})/A. \tag{3}$$

As shown in Table II, E_s accounts for a large part of the adhesive energy, even though the metal slab considered in this study consists of only three layers. While the chemical interaction is restricted adjacent to the interface as in Figs. 3 and 4, E_s arises from the long-range elastic interaction and would increase as a function of the number of metal layers.

TABLE II. Adhesive energies of Cu/MgO(001) and Ni/MgO(001).

	Model	E_c (J/m^2)	E_s (J/m^2)
Cu/MgO(001)	Incoherent	0.65	0.18
	Coherent (O-atop)	0.86	
	Coherent (Mg-atop)	0.06	
Ni/MgO(001)	Incoherent	0.96	0.34
	Coherent (O-atop)	1.93	
	Coherent (Mg-atop)	0.46	

Therefore, the effects of interfacial strain on the adhesive energy are more significant to evaluate the stability of incoherent interfaces between thicker metal and oxide layers. By inspection of Figs. 1(a) and 2(a), there are nine metal atoms displaced to the coherent O-atop positions. Considering energies to deform a metal slab of three layers to the MgO lattice constant, $1.20A_{\mathrm{int}}$ J for Cu and $2.19A_{\mathrm{int}}$ J for Ni in our DFT calculations, the value of E_s is reasonable in terms of the strained O-atop region of the incoherent interface. However, E_c is larger than weighted average of interface properties calculated for the symmetric coherent structures. The reason is the image-charge interaction induced above the Mg atoms is underestimated for the Mg-atop coherent structure.

IV. SUMMARY

In summary, we have investigated interface structure and adhesion behavior of incoherent metal/oxide interfaces with large misfit, Cu/MgO(001) and Ni/MgO(001), based on DFT. The interfacial strain and bonding characteristics are inhomogeneous, depending on local atomic configurations at the incoherent interfaces. In regions where a metal atom is located near an O atom, the misfit is compensated as the metal layer is stretched to the period of MgO. The adhesion behavior at the O-atop site has a covalent and an ionic bonding characteristic. On the other hand, in regions where a metal atom is situated near a Mg atom, there is little in-plane strain and the incoherent geometry is held. The metal-Mg adhesive interaction is mediated by the image-charge electron accumulation induced above the Mg atoms, which is absent in DFT results using the Mg-atop coherent structure. It is also shown that the effects of the interfacial strain as well as the metal-Mg interaction on the adhesive energy are significant. Although the results presented here are obtained for the incoherent interface between metal and perfect MgO layers, effects of defects such as oxygen vacancies on the adhesion behavior will be studied in our future work.

ACKNOWLEDGMENTS

This work is partly supported by the Ministry of Education, Culture, Sports, Science and Technology of Japan (MEXT), through their Grant-in-Aid for Scientific Research on Priority Areas, 15074214, and through their Grant-in-Aid for Young Scientists(B), 19760067.

*matsunaka@mech.eng.osaka-u.ac.jp

[1] *Metal-Ceramic Interfaces*, edited by M. Rühle, A. G. Evans, M. F. Ashby, and J. P. Hizth (Pergamon, Oxford, 1990); M. Rühle, J. Surf. Anal. **3**, 157 (1997).
[2] M. W. Finnis, J. Phys.: Condens. Matter **8**, 5811 (1996).
[3] F. Ernst, Mater. Sci. Eng., R. **14**, 97 (1995).
[4] G. Pacchioni and N. Rösch, J. Chem. Phys. **104**, 7329 (1996).
[5] N. López, F. Illas, N. Rösch, and G. Pacchioni, J. Chem. Phys. **110**, 4873 (1999).
[6] I. Yudanov, G. Pacchioni, K. Neyman, and N. Rösch, J. Phys. Chem. B **101**, 2786 (1997).
[7] A. Markovits, J. C. Paniagua, N. López, C. Minot, and F. Illas, Phys. Rev. B **67**, 115417 (2003).
[8] Y. F. Zhukovskii, E. A. Kotomin, and G. Borstel, Vacuum **74**, 235 (2004).
[9] Y. Wang, E. Florez, F. Mondragon, and T. N. Truong, Surf. Sci. **600**, 1703 (2006).
[10] S. Fernandez, A. Markovits, F. Fuster, and C. Minot, J. Phys. Chem. C **111**, 6781 (2007).
[11] J. B. Zhou, H. C. Lu, T. Gustafsson, and E. Garfunkel, Surf. Sci. **293**, L887 (1993).
[12] M.-C. Wu, W. S. Oh, and D. W. Goodman, Surf. Sci. **330**, 61 (1995).
[13] A. Barbier, G. Renaud, and O. Robach, J. Appl. Phys. **84**, 4259 (1998).
[14] C. T. Campbell and D. E. Starr, J. Am. Chem. Soc. **124**, 9212 (2002).
[15] C. Li, R. Wu, A. J. Freeman, and C. L. Fu, Phys. Rev. B **48**, 8317 (1993).
[16] T. Hong, J. R. Smith, and D. J. Srolovitz, Acta Metall. Mater. **43**, 2721 (1995).
[17] J. Goniakowski and C. Noguera, Interface Sci. **12**, 93 (2004).
[18] S. Fernandez, A. Markovits, F. Fuster, and C. Minot, J. Phys. Chem. C **111**, 6781 (2007).
[19] R. Benedek, A. Alavi, D. N. Seidman, L. H. Yang, D. A. Muller, and C. Woodward, Phys. Rev. Lett. **84**, 3362 (2000).
[20] K. Matsunaga, T. Sasaki, N. Shibata, T. Mizoguchi, T. Yamamoto, and Y. Ikuhara, Phys. Rev. B **74**, 125423 (2006).
[21] H. Bialas and K. Heneka, Vacuum **45**, 79 (1994).
[22] J. P. McCaffrey, E. B. Svedberg, J. P. Phillips, and L. D. Madsen, J. Cryst. Growth **200**, 498 (1999).
[23] P. E. Blöchl, Phys. Rev. B **50**, 17953 (1994).
[24] G. Kresse and D. Joubert, Phys. Rev. B **59**, 1758 (1999).
[25] G. Kresse and J. Furthmüller, Comput. Mater. Sci. **6**, 15 (1996).
[26] J. P. Perdew, J. A. Chevary, S. H. Vosko, K. A. Jackson, M. R. Pederson, D. J. Singh, and C. Fiolhais, Phys. Rev. B **46**, 6671 (1992).
[27] H. J. Monkhorst and J. D. Pack, Phys. Rev. B **13**, 5188 (1976).
[28] A. M. Stoneham and P. W. Tasker, J. Phys. C **18**, L543 (1985).
[29] M. W. Finnis, Acta Metall. Mater. **40**, S25 (1992).